Thin Solid Films 547 (2013) 141–145

Contents lists available at ScienceDirect

Thin Solid Films

journal homepage: www.elsevier.com/locate/tsf

Self-forming barrier characteristics of Cu–V and Cu–Mn films for Cu interconnects

Jae-Hyung Park [a], Dae-Yong Moon [a], Dong-Suk Han [a], Yu-Jin Kang [a], So-Ra Shin [b], Jong-Wan Park [b,*]

[a] Division of Nanoscale Semiconductor Engineering, Hanyang University, 17 Haengdang-dong, Seoungdong-ku, Seoul 133-791, Republic of Korea
[b] Division of Materials Science & Engineering, Hanyang University, 17 Haengdang-dong, Seoungdong-ku, Seoul 133-791, Republic of Korea

ARTICLE INFO

Available online 1 May 2013

Keywords:
Cu interconnection
Self-forming barrier
V
Mn

ABSTRACT

We investigated the influence of annealing on the diffusion barrier property in a Mn-based and V-based barrier layer. The samples were annealed at various temperatures for 1 h in vacuum. X-ray diffraction revealed Cu (111), Cu (200) and Cu (220) peaks for the Cu–Mn and Cu–V alloys. Transmission electron microscopy showed that a 4–7 nm V-based interlayer self-formed and a 2–5 nm Mn-based interlayer self-formed at the interface after annealing. The resistivity of the annealed Cu–V alloy was reduced to 8.1 μΩ-cm, which is greater than the resistivity of the annealed Cu–Mn alloy. The Mn-based interlayer and V-based interlayer showed excellent thermal stability. The results show that Mn and V based Cu alloys are suitable seed layer materials for Cu interconnects.

© 2013 Elsevier B.V. All rights reserved.

1. Introduction

Cu-based interconnects continue to be used in leading edge integrated circuits because of their low resistivity and improved electromigration resistance. A typical Cu metallization consists of a Cu seed layer physical vapor deposited on a Ta/TaN barrier, followed by electroplating Cu. However, in this type it is more difficult to form a continuous Cu seed layer with aggressive device shrinkage, resulting in void formation in the Cu interconnects [1,2].

In order to overcome this difficulty, adding small amounts of alloying elements to Cu has been suggested for the diffusion barrier characteristics, adhesion, electromigration and resistivity [3–9]. It has been reported that alloying with a strong oxide former, such as Mg or Al, can improve the adhesion of copper. Besides, after heat treatment, a thin oxide layer was formed on the film surface and acted as a self-passivation layer [7,10,11]. These sequences and mechanisms of the interface oxidation reaction were reported by Frederick et al. for Cu–Mg alloys. They investigated the formation of a uniform MgO layer 20 nm thick at the interface after 600 °C annealing [12–14]. Koike et al. also showed a self-forming process that was demonstrated by using a Cu–Mn alloy as the seed layer [3,15]. They chose Mn as the alloying element because of the following favorable characteristics of Mg and Al: the driving force for oxide formation at the interface; the standard free energy of the oxide formation of the Mn similar to that of SiO_2. The diffusivity of Mn in Cu is faster than the self-diffusivity of Cu by an order of magnitude at 450 °C [16]. Moreover, the activity coefficient of Mn in Cu is larger than 1 [17].

In this present work, we report a Cu–V alloy as well as a Cu–Mn alloy for the self-forming barrier process. The ΔG^o parameter of V oxide is slightly smaller than that of Mn at low temperature (<~1200 °C). The diffusivity of V is slightly lower in Cu compared to Mn [16]. Consequently, these two elements are investigated in terms of their barrier characteristics, resistivity, and interfacial reaction/diffusion between the Cu alloy and SiO_2.

2. Experimental details

Experiments were performed as follows. The alloy films of Cu-7.6 at.% V and Cu-9.1 at.% Mn were deposited directly onto the SiO_2 substrates to a thickness of 50 nm by simultaneous sputtering of Cu (99.99%) and alloy (99.99%) targets. The substrates were *n*-type Si wafers with SiO_2 100 nm in thickness. The distance between the targets and the substrate was ~5 cm. The substrate was rotated during deposition in order to obtain homogeneous concentration of the alloy film. The substrate was heated at 150 °C during deposition for the purpose of obtaining low resistivity of the alloy film. The chamber was evacuated down to 1.334×10^{-4} Pa as the base pressure, and a working pressure of 6.67×10^{-1} Pa was maintained with Ar gas. The RF power density was 1.38 W cm^{-2} on the Cu target and the RF power density was maintained at 0.91 W cm^{-2} on the alloy target. The deposition time was 5 min and the thickness of the pure Cu and Cu alloy thin film was about 50 nm. The samples were then annealed in a separate annealing chamber with a base pressure of 4.00×10^{-1} Pa. Annealing was carried out in a vacuum at various temperatures up to 400 °C for 1 h. High-resolution X-ray diffraction (XRD; Rigaku D/max-2500/pc, Cu-Kα = 1.54062 nm, Japan) analysis was applied to examine the crystal structure of the deposited thin film. Standard θ–2θ XRD measurements were performed at 40 kV and 30 mA. The film thicknesses, self-formed interlayer thickness,

* Corresponding author.
E-mail address: jwpark@hanyang.ac.kr (J.-W. Park).

0040-6090/$ – see front matter © 2013 Elsevier B.V. All rights reserved.
http://dx.doi.org/10.1016/j.tsf.2013.04.052

and the microstructures of the Cu alloy before and after annealing were analyzed using transmission electron microscopy (TEM; 300 kV, Hitachi HD-2300A). TEM samples were prepared by mechanical grinding and ion milling. For measuring the leakage current density of the Cu-alloy/SiO_2/Si, multilayer samples were formed by a lift-off process and the thermal stability of the copper diffusion barrier was tested. The metal-insulator-semiconductor (MIS) capacitor structures, Cu and Cu-alloy films were used as the gate electrodes. The electrode dot was 0.04 cm^2 and formed by a lift-off process. The leakage current densities versus electrical field (I–V) curves were measured by using a HP4145 picoammeter/dc voltage source with the electric field swept from zero to 0.7 MV/cm.

3. Results and discussion

The XRD diffraction patterns of the post-annealed Cu–V alloy/SiO_2/Si samples and the post-annealed Cu–Mn alloy/SiO_2/Si samples are shown in Fig. 1. There was no other detectable phase besides Cu (111), Cu (200), and Cu (220). Also, no binary Cu intermetallic compound was detected for thermal treatments up to 400 °C. Under severe annealing conditions, a failed Cu barrier allows the diffusion of a significant amount of Cu into the dielectric, forming a detectable Cu_3Si peak [18]. In our case, the annealing condition (1 h at 400 °C) probably was not severe enough to form silicide. Meanwhile, the Cu signals become sharper as the annealing temperature increases, indicating Cu grain growth at an elevated temperature. In addition, the strong increase of Cu (111) peak was detected after annealing. Wong et al. reported that a strong Cu (111) can enhance the adhesion between the Cu seed layer and the diffusion barrier [19]. The reaction rate for Cu oxide and Cu silicide can also be slowed down when for Cu exhibits (111) texture [20,21]. From this perspective, enhancing the

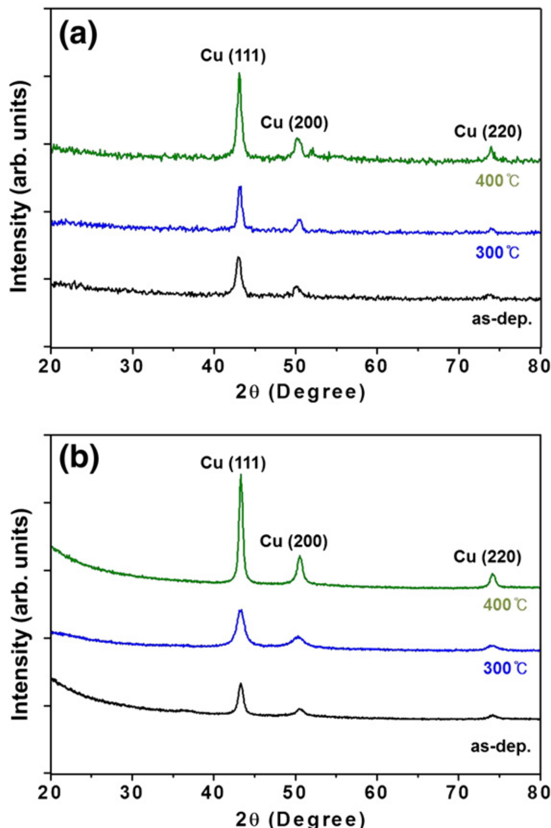

Fig. 1. X-ray diffraction (XRD) patterns of the (a) Cu–V alloy/SiO_2/Si and the (b) Cu–Mn alloy/SiO_2/Si at various annealing temperatures.

Cu (111) peak intensity in the Cu–V alloy/SiO_2/Si and Cu–Mn alloy/SiO_2/Si samples after annealing can be superior performance of the Cu interconnects.

The TEM micrographs on the surfaces of the Cu/SiO_2/Si, Cu–Mn alloy/SiO_2/Si and Cu–V alloy/SiO_2/Si samples, before and after annealing, are shown in Fig. 2. Before the annealing process, there is no significant difference in the surface morphology [Fig. 2(a), (c) and (e)]. However, after annealing, the grain boundaries of the Cu or Cu alloy films can be clearly observed due to the grain growth and the thermal grooving at the boundaries. As shown in Fig. 3(a)–(f), after annealing at 300 °C for 1 h, the grains had grown in size. The estimated grain sizes of the Cu, Cu–Mn and Cu–V alloy were 45, 41, and 25 nm, respectively. The grain size of the Cu–Mn alloy film is similar to the Pure Cu alloy film, while the Cu–V alloy film has a smaller grain size than the Pure Cu alloy film. This difference indicates that V has a smaller solute solubility than Mn. Therefore, the V atoms may segregate to the grain boundaries and hinder the movement of the grain boundaries. Consequently, the degree of grain growth is less in the Cu–V alloy than in the others.

The resistivity of the pure Cu, Cu–Mn alloy and Cu–V alloy films was measured with the four-point probe method, as shown in Fig. 3. In comparing the resistivity of the films, which were measured after annealing them for 1 h at various temperatures, the resistivity of as deposited Cu, Cu–Mn, and Cu–V alloy films were approximately 4.2, 12.1 and 13.4 μΩ-cm, respectively. After annealing at 300–400 °C, the resistivity of all the samples decreased. In general, the sheet resistance gradually decreases to some extent as the annealing temperature increases due to the grain growth. The slight reduction in resistivity for the pure Cu film suggests defect annihilation and grain growth. The reduction in the resistivity was the most significant for the Cu-alloy films. It can be attributed to the grain growth, segregation and out-diffusion of the alloy content. However, the resistivity of the Cu–V alloy films is still high at about 8.1 μΩ-cm. It indicates that annealed Cu–V alloy films may contain residual V or lattice defects after annealing. In addition, the annealed Cu–V alloy has higher density of grain boundary than in the others. Because of electron scattering caused by grain boundary, the resistivity of annealed Cu–V alloy is still greater than that of pure Cu and Cu–Mn alloy. This behavior corresponds to the TEM micrograph (Fig. 2f).

Fig. 4 shows the cross-sectional TEM images of the Cu–V alloy/SiO_2/Si and Cu–Mn/SiO_2/Si samples annealed at 300–400 °C for 1 h. All of the magnified images clearly show the formation of a nanoscale interface layer with an approximate thickness of 2.5 and 4 nm of the Cu–Mn alloy, and 4.5 and 7 nm of the Cu–V alloy, respectively. At the interface between Cu and the SiO_2, the formation of an ultrathin layer appears. The morphology of the V-based interlayer and the Mn-based interlayer with a thickness of 2–7 nm was found to be uniform at the interface. In addition, at the same annealing temperature, the V-based interlayer had a thicker interlayer than the Mn-based interlayer. The V-based interlayer thickness was larger than the Mn-based interlayer thickness, possibly because of the logarithmic rate law that is the mechanism of metal oxide formation. The low temperature oxidation is based on the assumption of an electron or hole tunneling through an initially thin oxide of less than approximately 10 nm in thickness. Under this assumption, a potential drop occurs across the oxide caused by the difference between the work function of the metal and the chemical affinity of oxygen. The resulting electric field across the oxide layer can serve as a driving force for ionic transport, which is considered to be the rate-controlling process of oxide growth. This indicates that the growth of the barrier layer occurs by the field-enhanced ionic transport. Once Mn and V ions diffuse into SiO_2, the barrier layer is formed and its growth is rate-controlled by ion diffusion through the barrier layer [20–22]. Although Mn had higher diffusivity in the Cu, the strength of the electric field between both sides of the V-based

Download English Version:

https://daneshyari.com/en/article/1665905

Download Persian Version:

https://daneshyari.com/article/1665905

Daneshyari.com